Engineering Failure Analysis 101 (2019) 485–492

Contents lists available at ScienceDirect

Engineering Failure Analysis

journal homepage: www.elsevier.com/locate/engfailanal

Failure of polymer coated nylon parts produced by additive manufacturing

M. Miguel[a], M. Leite[b], A.M.R. Ribeiro[a], A.M. Deus[c], L. Reis[a], M.F. Vaz[a,*]

[a] IDMEC, Instituto Superior Técnico, Universidade de Lisboa, 1049-001 Lisboa, Portugal
[b] UNIDEMI, Departamento de Engenharia Mecânica e Industrial, Faculty of Science and Technology, New University of Lisbon, Portugal
[c] CEFEMA, Instituto Superior Técnico, Universidade de Lisboa, Lisboa, Portugal

ARTICLE INFO

Keywords:
Polymers
Fused deposition modelling
Mechanical properties
Damage
Failure

ABSTRACT

Fused deposition modelling (FDM) shows a great potential for the production of complex shapes in the case of several materials including nylon, which is a type of polyamide. In such materials, water absorption is an issue that requires attention and there is interest in studying the application of protective products, with the goal of improving the sealing properties of the parts.

The objective of this work is to analyze and evaluate the water absorption, mechanical properties and consequent failure surfaces of nylon parts obtained by FDM, with two raster angles, after being coated with a protective material. Two polymeric products were used to coat the parts, polyurethane elastomer and silicone.

The performance of the coated parts was evaluated with water absorption tests, as well as compression and tensile tests. The treatment was found to reduce the open porosity and to decrease the mechanical properties of the specimens in different raster angles. Failure occurs at surfaces making angles of zero or forty five degrees from the applied force, depending on the raster angle, both in treated and untreated samples.

1. Introduction

In recent times, fused deposition method (FDM) has become one of the most common additive manufacturing techniques. The advantages of FDM rely on the production of complex shapes with reductions of time and cost for prototypes and small series [1–3]. FDM techniques are promising fabrication methods for biomedical devices, such as implants, prosthesis or scaffolds for tissue engineering among other fields of application.

In FDM, a thermoplastic material is extruded by a temperature-controlled head with a nozzle. The nozzle is fed by a filament of material that is unwound from a coil, and the material is heated to a semi-molten state, being deposited on the constructed part. The polymer fuses with the material that has already been deposited. The part is fabricated layer by layer with the system operating in the X, Y, and *Z*-axes according to the computer-aided design. The nozzle moves into the X-Y plane to draw the part and moves in the Z plane to deposit new layers. In general, the system is placed inside a chamber held at a temperature below the melting point of the polymer, but warm enough to avoid excessive temperature gradients in the part being built [4].

The part building direction, bead width, air pockets, raster angle, layer thickness, number of contours and temperature are among the most important factors in the FDM process [2,3,5]. The build direction is defined as the direction perpendicular to the plane of the layer or of the tray, while the raster angle is the angle between the roads of material relative to a reference direction [2,5]. The FDM

* Corresponding author.
E-mail address: fatima.vaz@tecnico.ulisboa.pt (M.F. Vaz).

https://doi.org/10.1016/j.engfailanal.2019.04.005
Received 30 January 2019; Received in revised form 20 March 2019; Accepted 2 April 2019
Available online 03 April 2019
1350-6307/

process begins with a deposition along the part contour, after which the material is deposited at the inner side of the external layer.

Due to the directional deposition of material, FDM parts exhibit an anisotropic behavior. This has been verified by several authors who have studied the mechanical properties of FDM parts [2,6,7].

The most common polymers that are used in the FDM process are ABS (acrylonitrile butadiene styrene), PMMA (poly(methyl methacrylate)), PCL (poly(e-caprolactone)), PLA (polylactic acid), PLGA (poly(lactidecoglycolide)) [5–10]. Nylon or polyamide is a biocompatible polymer with acceptable mechanical properties and excellent processability by FDM. Nylon may be used in automotive parts [11], and has potential to be employed in medical implants [12]. Though nylon shows attractive physical and mechanical properties, a disadvantage is the fact that it absorbs humidity with a consequent reduction of strength and stiffness [11].

Frequently, surface finish treatments are applied to printed parts by complex procedures, such as, vacuum infiltration or with simpler methods, such as brushing [13]. The treatments with sealants or protective products may reduce the water absorption or increase the pressure that a part will withstand [7,13], widening its range of application. However, an optimal treatment must preserve the dimensions of the specimens, which is not the case, for example, of acetone treatments [7]. Also protective products must be chosen without environmental and health risks.

Polyurethane based coatings have a wide spectrum of applications because of their remarkable properties resulting from intermolecular hydrogen bonds among urethane linkages of polymer molecules [14]. Polyurethane products are among the leading coating materials, as they possess high thermal and chemical stability, resistance in aggressive environments, easy applicability and the fact that its usage is consistent with good sustainability of the parts [14].

The usage of silicone coatings is widespread ranging from domestic applications to construction [15,16]. They have the ability to bind different materials such as glass, metal or plastics due to the formation of very stable chemical bonds at the surfaces. This type of coating provides inertness against chemical attacks, as well as anti-corrosion and anti-biofouling capacities [15,16].

A major drawback of FDM is the poorly bonded adhesion between layers, and the formation of small porosities [12]. Since the FDM technique has numerous advantages, research has been concentrated on improving the material performance and functionality.

To our knowledge, the literature on the modification of polyamide surfaces of FDM parts is scarce. A treatment that fills the voids and reduces the porosity of FDM printed objects is of utmost importance. In the present work, attention is given to the coating of nylon FDM parts with polymeric products that provide reductions of the water absorption ability, which may broaden the field of nylon applications. The water absorption and mechanical properties of polyamide FDM parts coated with two protective products, polyurethane elastomer and silicone, were studied. Two different raster angles were studied.

2. Materials and methods

Nylon parts were fabricated by FDM, with two distinct raster angles, after which a coating polymer was applied. Water absorption tests enable to assess the porosity before and after treatment, while the mechanical properties were evaluated by compressive and tensile tests. Failure analysis was undertaken on untreated and treated samples after performing tensile testing.

2.1. Materials

The specimens were created with the 3D CAD program Solidworks (SolidWorks, 2002). After being processed by the cloud-based software (EIGER, 2018) parts were printed in a Mark II device from Markforged. The material used was trademarked polyamide from the company Markforged. The temperature attained during extrusion was 280 °C and the layer thickness was 0.1 mm.

For the water absorption and compressive tests, cube samples with edge length of 10.05 ± 0.12 mm were printed (Fig. 1(a)). All the cubic specimens were built along the Z axis, perpendicular to the deposition tray, while the raster angle was 0° or 45°. As in previous work [7] samples will be designated by the build direction and the raster angle. According to this designation cubic samples will be denoted by (Z, 0) and (Z, 45). Tensile specimens were produced according to the ASTM D638-14 standard [17] (Fig. 1(b)) and, according to previous designations, will be denoted by (Y, 0) and (Y, 45).

Two coating polymers were studied: a polyurethane elastomer 10Excellent (CPP Chemical Group, Spain) and liquid silicone Rubson SL 3000 (Henkel Iberica, Portugal). Both products are used in outdoor water proof applications, such as roofs and terraces protection. Treated samples will be denoted by *Exc* or *Rub* in accordance to the name of the polymeric product. The protective products were used as received from the supplier. Two brushing treatments of the coating product were applied to each specimen, as

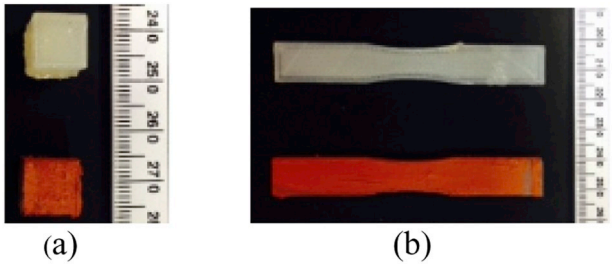

Fig. 1. Specimens coated with *Exc* and *Rub* products: (a) compression samples; (b) tensile samples.

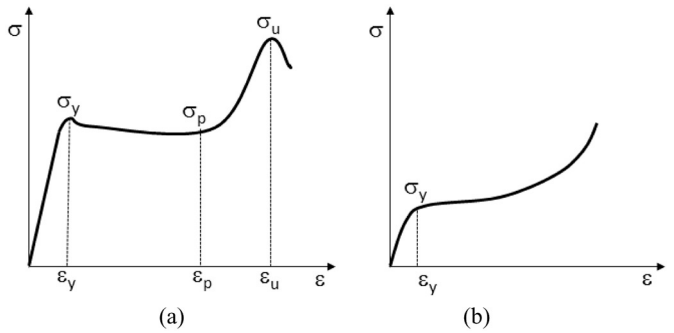

Fig. 2. Scheme of stress-strain curves obtained under: (a) tensile and (b) compressive tests.

recommended by the supplier. For the same testing conditions, at least three specimens were studied.

2.2. Experimental tests

2.2.1. Water absorption

The water absorption tests were conducted according to the standard ASTM D570 [18] for both coated and uncoated specimens. After being dried at 50 °C for 24 h, the samples were cooled at room temperature and placed over a filter paper pile immersed in water until 24 h or weight equilibrium is achieved. The specimens were periodically removed from the water, and weighed.

The designations adopted are m_{dry} for the dry mass, m_{wet} for the wet mass and m_{sat} which is the weigh achieved at the end of the test. The plots of the difference between the wet and dry mass per unit area of the sample surface as a function of the square root of the immersion time represent the water absorption curves. From the slope of the initial part of the curves, the absorption coefficient, *A*, was estimated. The maximum water content, *CI*, and the open porosity, *op*, were determined, as in a previous study [7], respectively, by

$$CI\ (\%) = \frac{m_{sat} - m_{dry}}{m_{dry}} \times 100 \tag{1}$$

$$op\ (\%) = \frac{(m_{sat} - m_{dry})/\rho_{water}}{V} \times 100 \tag{2}$$

where ρ_{water} is the water density and *V* is the volume of the sample.

2.2.2. Mechanical tests

Compression and tension tests were conducted on an Instron 3369 universal testing machine with a load cell of 10 kN and a cross-head speed of 2.5 mm/min in compression and 10 mm/min in tension. At least three tests were conducted under the same conditions. For each test, the load-displacement data was used to obtain the stress-strain curves using the Bluehill Software. Load was applied in the Z direction for compression tests and in the Y direction during tensile experiments.

The yield stress σ_Y and strain ε_Y, the plateau stress σ_p and strain ε_p, and the ultimate stress σ_u and strain $\varepsilon_u$were acquired from the tensile curves, as depicted in Fig. 2(a). The slope of the initial part of the curve, E, was also determined. From the compression results, the yield stress σ_Y and yield strain ε_Y were recorded (Fig. 2(b)), as well as, the slope of the initial region, *E*.

After performing tensile tests, the failure surfaces were observed in an optical microscope in order to evaluate the failure mechanisms.

3. Results and discussion

Water absorption tests were conducted to assess the effectiveness of the coating treatment in reducing the porosity. The mechanical properties of the specimens were determined by compression and tensile tests.

The coating thickness of the specimens was measured with the help of image analysis software. The coating thicknesses of samples treated with the *Rub* product and with the *Exc* product were found to be, respectively, 0.265 ± 0.076 mm and 0.215 ± 0.061 mm.

Table 1
Water absorption properties of specimens untreated and treated with *Exc* and *Rub* products.

Treatment	*CI* (%)	*op* (%)	*A* ($g\,cm^{-2}\,min^{-1/2}$)
UT (untreated)	5.04 ± 0.56	5.27 ± 0.04	$3 \times 10^{-4} \pm 4 \times 10^{-5}$
Exc	2.05 ± 0.09	2.37 ± 0.50	$3 \times 10^{-4} \pm 1 \times 10^{-5}$
Rub	2.54 ± 0.17	2.74 ± 0.18	$4 \times 10^{-4} \pm 2 \times 10^{-5}$

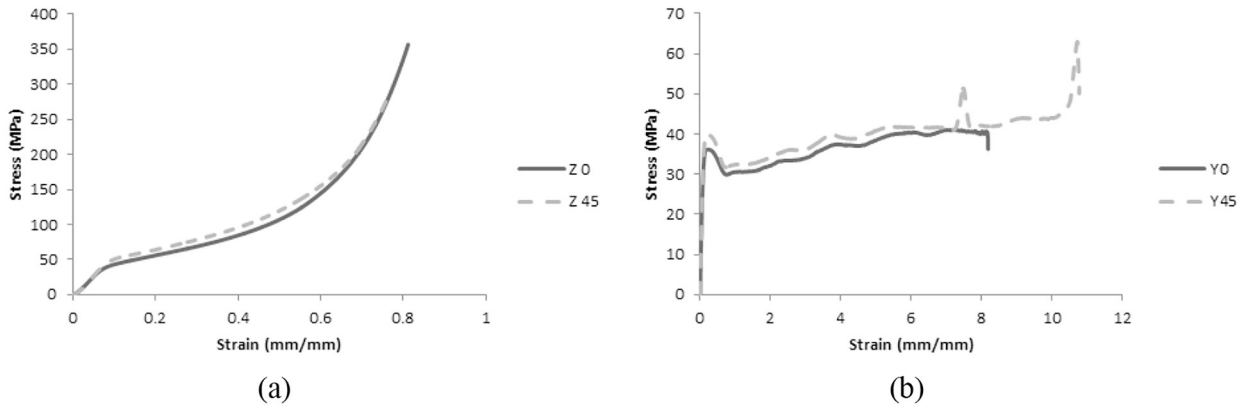

Fig. 3. Stress-strain curves obtained, for untreated specimens, under: (a) compression of cubic specimens (Z, 0) and (Z, 45) and (b) tension of specimens (Y, 0) and (Y, 45).

This means that the applied coating thickness is similar in both products.

The density of the uncoated nylon FDM parts was 1.05 ± 0.02 g/cm^3. Other characteristics, such as open porosity and mechanical properties of the untreated samples are given below and are compared with the coated samples results.

3.1. Water absorption

The average and standard deviation results of the parameters *CI*, *op* and *A* are indicated in Table 1, for untreated and treated cubic specimens (Z, 0).

Although the absorption coefficient *A* remains constant or increases, both protective polymers were found to reduce the water parameters *CI* and *op*, being effective concerning water absorption.

Although the use of silicone is recognized to lead to good weather resistance properties to nylon [19], the *Rub* product poorly adheres to the polyamide specimens.

In comparison with *Rub* product, the polyurethane *Exc* product presented almost the same values of the water parameters, *CI* and *op*. However, the surface treatment with the *Exc* product provides a coating adherent to the polyamide part.

Nylon or polyamide possess a polar structure that attracts moisture, due to the bonding established with the hydrogen in the water molecule [11]. However, polyamide in the presence of polyurethane, accomplish hydrogen bonding taking place among the coating molecules [20], which, consequently, prevents the formation of bonding with the water molecules, which, in turn, will reduce the water absorption.

Polyurethane sealer was previously applied to ABS printed 3D parts [7], but the results were not so promising as in the case of the present work.

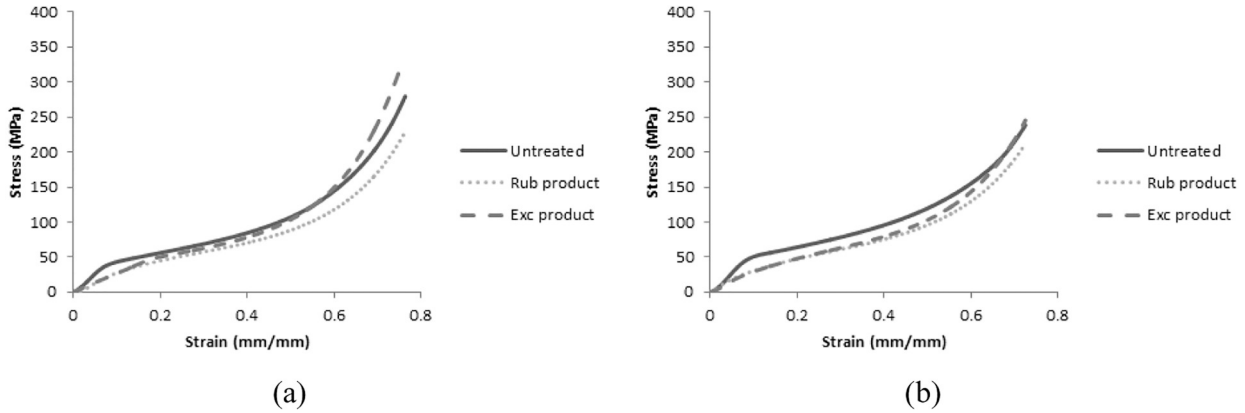

Fig. 4. Compression stress-strain curves of cubic specimens submitted to protective treatments with *Rub* and *Exc* products, which are compared to the untreated specimens. Two raster angles of 0° and 45° were evaluated, respectively, in the samples (a) (Z,0) and (b) (Z,45).

Table 2
Compression results for specimens (Z, 0) and (Z, 45).

Raster angle	Sample	ε_Y (mm/mm)	σ_Y (MPa)	E (MPa)
0°	UT	$5.5 \times 10^{-2} \pm 7.3 \times 10^{-3}$	31.29 ± 1.96	442.54 ± 41.26
	Exc	$1.7 \times 10^{-1} \pm 1.7 \times 10^{-2}$	23.53 ± 2.97	284.64 ± 16.62
	Rub	$7.8 \times 10^{-1} \pm 1.7 \times 10^{-2}$	19.94 ± 3.07	271.88 ± 35.94
45°	UT	$5.9 \times 10^{-2} \pm 5.9 \times 10^{-3}$	36.72 ± 1.31	402.39 ± 32.96
	Exc	$6.2 \times 10^{-2} \pm 8.5 \times 10^{-3}$	16.92 ± 0.38	309.68 ± 20.76
	Rub	$4.3 \times 10^{-2} \pm 1.1 \times 10^{-3}$	13.87 ± 1.85	303.93 ± 22.32

Table 3
Results obtained in the tension tests of specimens untreated and submitted to a treatment with *Rub* and *Exc* products for two raster angles.

Sample	ε_Y (%)	σ_Y (MPa)	E (MPa)	ε_p (%)	σ_p (MPa)	ε_u (%)	σ_u (MPa)
Untreated							
Y0	0.164 ± 0.037	35.83 ± 1.02	323.62 ± 21.33	7.09 ± 3.45	38.91 ± 3.10	–	–
Y45	0.127 ± 0.020	38.29 ± 0.14	357.11 ± 14.17	10.18 ± 0.23	43.64 ± 0.44	10.61 ± 0.10	59.08 ± 5.55
Treated							
Exc Y0	0.408 ± 0.028	28.69 ± 0.50	215.94 ± 16.64	7.72 ± 0.30	36.79 ± 0.59	9.22 ± 0.09	48.98 ± 1.13
Exc Y45	0.395 ± 0.016	26.94 ± 0.48	198.55 ± 8.58	7.39 ± 0.27	34.80 ± 0.77	9.10 ± 0.22	48.51 ± 0.81
Rub Y0	0.522 ± 0.171	28.16 ± 1.42	188.08 ± 14.06	6.32 ± 1.99	37.77 ± 0.56	8.11 ± 1.33	46.35 ± 2.35
Rub Y45	0.414 ± 0.022	28.03 ± 0.35	189.78 ± 5.64	7.34 ± 0.28	36.89 ± 1.38	9.27 ± 0.08	49.47 ± 0.24

3.2. Mechanical tests

3.2.1. Compression tests

Although three specimens were evaluated for each condition, only one curve is exhibited in the next figures. Average and standard deviation values will also be presented.

Fig. 3(a) exhibits an example of the stress-strain curves obtained under the compression of samples (Z, 0) and (Z, 45), without any coating. The effect of the raster angle in the compressive mechanical behaviour is negligible. Also, the curves of Fig. 3(b) attained with tensile tests of untreated specimens (Y, 0) and (Y, 45) are almost coincident until the plateau stress, being different after that zone.

Stress-strain curves of Fig. 4 were obtained in compression experiments of cubic specimens coated with *Rub* and *Exc* products. Also curves belonging to untreated specimens are shown in the figures. Specimens were printed with raster angles of 0° and 45°.

The parameters yield stress σ_Y, yield strain ε_Y and the slope of the initial region E, are presented in Table 2. Specimens printed with two different raster angles show some differences in the mechanical parameters, which leads to the conclusion that there is an anisotropy effect associated with the printed raster angle.

Results allow inferring that the coating treatments with polyurethane and silicone not only induce surface modifications, but also affect the bulk properties of the nylon specimens. A decrease in the values of yield stress and Young's modulus, and consequently a reduction of strength and stiffness was detected.

Although the application of polyurethane coatings on polyamide parts is not well documented, several studies in the literature focused on the copolymers of polyurethane soft segments in molecular chains of polyamide [21]. There is a strong interaction between the urethane group of the polyurethane and the amide group of nylon. When increasing the soft phase there is a decrease in the crystallinity of the copolymer, leading to lower mechanical properties [21]. A similar mechanism may explain the reduction of the mechanical properties in the coated samples.

3.2.2. Tensile tests

The specimens designated by (Y, 0°) and (Y, 45°) were coated with the polyurethane and silicone products and subjected to tensile tests. The parameters yield stress σ_Y and strain ε_Y, the plateau stress σ_p and strain ε_p, and the ultimate stress σ_u and strain ε_u are shown in Table 3.

The stress-strain curves (Fig. 5(a) and (b)) for specimens treated with *Rub* and *Exc* products show, for the two raster angles, a decrease in the yield and plateau stress in comparison with the untreated specimens. Both products give rise to very similar mechanical behavior as the stress-strain curves almost overlap. The reduction in the mechanical properties may be explained, as previously done for the compressive behavior, due to the bonding of polymeric groups.

The tensile curves revealed high ductility due to a good adhesion of the nylon thread lines that adhere to each other to build a layered printed part.

The tensile curves of printed polyamide parts are similar to the ones reported for pure nylon [12] and are different from the printed ABS parts [7]. The tensile yield stress of nylon is superior to the corresponding stress of ABS, while compressive yield stress of nylon is similar to the one of ABS parts [7].

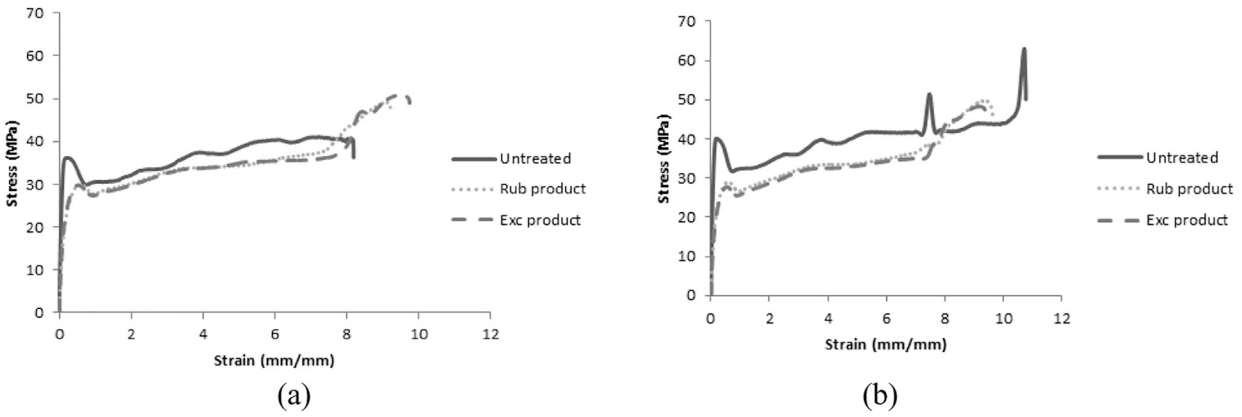

Fig. 5. Tensile stress-strain curves for untreated nylon specimens and treated with *Rub* and *Exc* products for samples: (a) (Y, 0) and (b) (Y, 45).

Fig. 6. Failure surfaces of tensile specimens coated with: *Rub* product (a) (Y, 0); (b) (Y, 45) and *Exc* product (c) (Y, 0); (d)(Y, 45).

3.3. Failure observations

Fig. 6 exhibits the specimens coated with the *Rub* and the *Exc* product after being subjected to tensile tests. The poor adhesion of the *Rub* coating is notorious. Both treated samples exhibited angles of fracture of 0° or 45° which are coincident with the printed raster angles, which mean that the failure angle is not affected by the surface treatment.

Fig. 7 helps to understand the failure mechanism, as adjacent layers remain aligned after deformation and fail in accordance with the printed angle. In the case of the samples coated with the *Exc* product, the resolution of the image is not very good.

The mechanism of deformation involves several steps starting with an initial phase where the distance between adjacent layers is the same all over the specimen. After the yield stress, there is the formation of a deformation band, where the distance between layers is higher than outside the band. During the plateau zone of the stress-strain curves, the deformation band propagates along the specimen. After the plateau phase, the stress increases until the ultimate stress is attained, which correspond to the separation of the sample in two pieces.

4. Conclusions

The fact that nylon is hygroscopic (i.e. moisture sensitive) needs to be taken into account in materials selection and design, as mechanical properties of parts made from this polymer are affected by water.

The results of the present paper indicate that coating FDM parts with polyurethane based products enables to obtain polyamide parts with reduced water absorption properties, which will provide a larger range of applications. The coating parts present lower strength and stiffness in comparison with the untreated specimens, but still show acceptable mechanical properties for non-load bearing applications.

Specimen fail at surfaces that make angles with the applied loads that are coincident with the printed raster angles. The coating does not affect the failure mechanism of nylon parts.

Surface modification of nylon 3D printed parts allows for new applications where sealing is seen as an important factor.

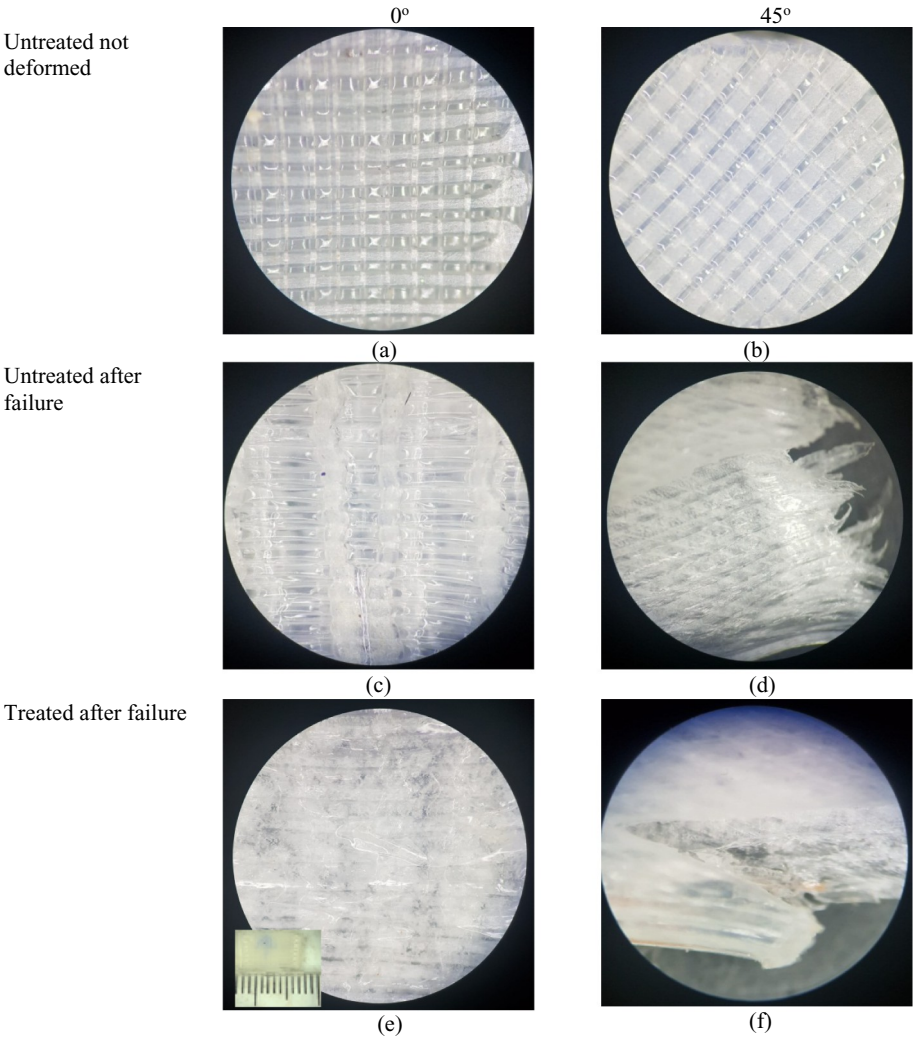

Fig. 7. Structure of tensile nylon parts for raster angles of 0° and 45°, respectively, for (a), (b) untreated not deformed; (c), (d) untreated after failure, and (e), (f) treated with *Exc* product after tensile tests. (Scale – distance between longer lines equals to 10 mm).

Acknowledgements

This work was supported by Fundação para a Ciência e Tecnologia (FCT), Portugal, through IDMEC, under LAETA, project UID/EMS/50022/2019. Acknowledgements are due to Manuel Sardinha, Pedro Costa and Henrique Soares.

References

[1] D. Um, Rapid Prototyping, Solid Modeling and Applications, Springer International Publishing, Cham, 2016.
[2] D. Croccolo, M. De Agostinis, G. Olmi, Experimental characterization and analytical modelling of the mechanical behaviour of fused deposition processed parts made of ABS-M30, Comput. Mater. Sci. 79 (2013) 506–518, https://doi.org/10.1016/j.commatsci.2013.06.041.
[3] B.N. Turner, R. Strong, S.A. Gold, A review of melt extrusion additive manufacturing processes: I. process design and modelling, Rapid Prototyp. J. 20 (2014) 192–204, https://doi.org/10.1108/RPJ-01-2013-0012.
[4] S.S. Crump, Apparatus and Method for Creating Three-Dimensional Objects., US Pat. 5,121,329. (1992).
[5] C.S. Lee, S.G. Kim, H.J. Kim, S.H. Ahn, Measurement of anisotropic compressive strength of rapid prototyping parts, J. Mater. Process. Technol. 187–188 (2007) 627–630, https://doi.org/10.1016/j.jmatprotec.2006.11.095.
[6] B.M. Tymrak, M. Kreiger, J.M. Pearce, Mechanical properties of components fabricated with open-source 3-D printers under realistic environmental conditions, Mater. Des. 58 (2014) 242–246, https://doi.org/10.1016/j.matdes.2014.02.038.
[7] M. Leite, A. Varanda, A.R. Ribeiro, A. Silva, M.F. Vaz, Mechanical properties and water absorption of surface modified ABS 3D printed by fused deposition modelling, Rapid Prototyp. J. 24 (2018) 195–203, https://doi.org/10.1108/RPJ-04-2016-0057.
[8] C. Polzin, S. Spath, H. Seitz, Characterization and evaluation of a PMMA-based 3D printing process, Rapid Prototyp. J. 19 (2013) 37–43, https://doi.org/10.1108/13552541311292718.
[9] M. Vaezi, H. Seitz, S. Yang, A review on 3D micro-additive manufacturing technologies, Int. J. Adv. Manuf. Technol. 67 (2013) 1721–1754, https://doi.org/10.1007/s00170-012-4605-2.

[10] W. Wu, P. Geng, G. Li, D. Zhao, H. Zhang, J. Zhao, Influence of layer thickness and raster angle on the mechanical properties of 3D-printed PEEK and a comparative mechanical study between PEEK and ABS, Materials (Basel) 8 (2015) 5834–5846, https://doi.org/10.3390/ma8095271.
[11] N. Jia, H.A. Fraenkel, V.A. Kagan, Effects of moisture conditioning methods on mechanical properties of injection molded nylon 6, J. Reinf. Plast. Compos. 23 (2004) 729–737, https://doi.org/10.1177/0731684404030730.
[12] T.N.A.T. Rahim, A.M. Abdullah, H. Md Akil, D. Mohamad, Z.A. Rajion, The improvement of mechanical and thermal properties of polyamide 12 3D printed parts by fused deposition modelling, Express Polym Lett 11 (2017) 963–982, https://doi.org/10.3144/expresspolymlett.2017.92.
[13] J. Mireles, A. Adame, D. Espalin, F. Medina, R. Winker, T. Hoppe, B. Zinniel, R. Wicker, Analysis of sealing methods for FDM-fabricated parts, Solid Free. Fabr. (January 2011) 185–196.
[14] H.M.C.C. Somarathna, S.N. Raman, D. Mohotti, A.A. Mutalib, K.H. Badri, The use of polyurethane for structural and infrastructural engineering applications: a state-of-the-art review, Constr. Build. Mater. 190 (2018) 995–1014, https://doi.org/10.1016/j.conbuildmat.2018.09.166.
[15] V. Anoop, S. Subramani, S.N. Jaisankar, C. Sohini, N.L. Mary, Mechanical, dielectric, and thermal properties of polydimethylsiloxane/polysilsesquioxane nanocomposite for sealant application, J. Appl. Polym. Sci. 136 (2019) 47228, , https://doi.org/10.1002/app.47228.
[16] U. Eduok, O. Faye, J. Szpunar, Recent developments and applications of protective silicone coatings: a review of PDMS functional materials, Prog. Org. Coatings 111 (2017) 124–163, https://doi.org/10.1016/j.porgcoat.2017.05.012.
[17] ASTM D638 - 14, Standard Test Method for Tensile Properties of Plastic, (2014).
[18] ASTM D570-98, Standard Test Method for Water Absorption of Plastics, ASTM Stand, 2010, https://doi.org/10.1520/D0570-98R10E01.2.
[19] H. Bin Ou, M. Sahli, T. Barrière, J.C. Gelin, Adhesion strength study of silicone rubber compounds to nylon 66, Key Eng. Mater. 622–623 (2014) 453–458, https://doi.org/10.4028/www.scientific.net/KEM.622-623.453.
[20] C.-F. Ouyang, X.-T. Ji, Q. Gao, C.-Y. Xu, Modification of regeneration polyurethane by blend with ternary nylon, Proc. 2015 Int. Conf. Mater. Sci. Appl, Atlantis Press, Paris, France, 2015, , https://doi.org/10.2991/icmsa-15.2015.99.
[21] E.A. González-De Los Santos, A.S. López-Rodríguez, M.J. Lozano-González, F. Soriano-Corral, Starlike nylon 6/polyurethane block copolymers by reaction injection-molding process (RIM), J. Appl. Polym. Sci. 80 (2001) 2483–2494, https://doi.org/10.1002/app.1356.